Synsint Research Group

Available online at www.synsint.com

Synthesis and Sintering

ISSN 2564-0186 (Print), **ISSN** 2564-0194 (Online)

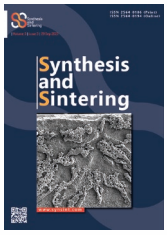

Review article

Microwave sintering of ZrB_2-based ceramics: A review

Samira Savani [a,*], **Mohammad Alipour** [b], **Ankur Sharma** [c], **Dagarapu Benny Karunakar** [c]

[a] *Otto Schott Institute of Materials Research, Friedrich Schiller University, Jena, Germany*
[b] *Volvo Trucks Technology, Eketrägatan 25, Göteborg, Sweden*
[c] *Mechanical and Industrial Engineering Department, Indian Institute of Technology Roorkee, 247667, India*

A B S T R A C T

Recently, microwave sintering has absorbed remarkable attention on the basis of enhanced microstructural/mechanical characteristics in comparison with conventional sintering techniques based on powder technology. This method not only can be employed for the processing of metals, alloys, and metal matrix composites but also for the manufacturing of advanced ceramics and ceramic matrix composites. Zirconium diboride (ZrB_2) as an interesting member of ultrahigh temperature ceramics is one of the most undertaking candidates in modern structural ceramics applications. This paper reviews the processing-densification-mechanical properties correlations in microwave-sintered ZrB_2-based ceramics and composites. The text concentrates on the microwave-assisted production of ZrB_2 divided into two categories: synthesis of ZrB_2 powders by microwave sintering and sintering of ZrB_2-based ceramics and composites by microwave sintering. The effects of some additives and reinforcements, such as B_4C, SiC, TiC, and MgO, on zirconium diboride's densification and mechanical properties are summarized.

KEYWORDS

Ultrahigh temperature ceramics
Microwave sintering
Synthesis
ZrB_2
Ceramic matrix composites

OPEN ACCESS

1. Introduction

Within the field of structural ceramics, specifically, aviation and defense sectors, nuclear reactors, and other routine applications such as thermal plants, refractory crucibles, and cutting apparatuses, efficiency is basically directed by homogeneous microstructure, low defects/pores and high density, uniform distribution of the secondary phases in the matrix [1, 2].

In recent decades, a new encouraging route has prospected within the carbides (ZrC, TaC, etc.), borides (HfB_2, ZrB_2, TiB_2, etc.), and nitrides (TaN, ZrN, HfN, etc.) of transition metals named ultra-high temperature ceramics (UHTCs) [3, 4]. UHTCs have inimitable combos of physical, mechanical, and tribological characteristics at elevated temperatures, comprising high thermal/electrical conductivity, chemical inertness to corrosive conditions, superb melting point, high hardness, and excellent thermal shock resistance [5–8]. Hence, these ceramics are the most suitable candidates molten metal crucibles, plasma electrodes, solar absorbers, and especially the production of components of thermal protection systems for hypersonic and re-entry atmospheric vehicles capable of withstanding severe flow conditions [9–11].

Among the members of the UHTC family, ZrB_2 has a reasonable price and an interesting mix of properties including chemical inertness, relatively low density, resistance to oxidation especially under adverse conditions, and good mechanical properties [4, 5]. Its structure consists of alternating Zr and B planes in a hexagonal P6/mmm symmetry [12]. ZrB_2 is predominantly covalent in nature, consists of covalent B–B bonds, metallic Zr–Zr bonds, and covalent/ionic Zr–B bonds, and also has a low rate of self-diffusion [13–16]. The formation of surface

* Corresponding author. *E-mail address:* samira.savani@uni-jena.de (S. Savani)
Received 20 November 2022; Received in revised form 28 July 2023; Accepted 29 July 2023.

https://doi.org/10.53063/synsint.2023.33129

oxides (B_2O_3 and ZrO_2) on ZrB_2 powder particles causes special problems in the sintering and condensation process [17, 18].

To fabricate dense and low-porosity ZrB_2 samples, ceramic powders should be sintered at high temperatures and preferably under pressure [19, 20]. The hot-pressing process is one of the most important methods, which of course has limitations, for example, this technique takes more time and therefore consumes a lot of electricity or it is limited to making parts with simple and uncomplicated shapes [21, 22]. Long heating and dwell time causes microstructure coarsening in the sintered samples, which negatively affects mechanical properties [23, 24]. To overcome such problems, new methods such as spark plasma sintering [25–27], laser sintering [28], and microwave sintering (please see next section) have been developed to help achieve maximum relative density and improve properties.

This review paper consists of two main parts. In the first part, the principles and definition of the microwave sintering process are provided, and in the second part, the effects of sintering variables and the introduction of additives, sintering aids, and secondary phases on the relative density and mechanical properties of ZrB_2 ceramics are discussed.

2. Basics of microwave sintering

The microwave sintering process was first proposed by Ford and Pei in 1967 at the Stanford University 2nd Symposium on Microwave Power [29]. The major advantage of the microwave sintering technique is the rapid and uniform heating of the sample because the energy required to sinter the powder particles is coupled directly to the sample rather than coming from an external source [30]. Fig. 1 shows the schematic sketch of the microwave sintering process [31]. In general, increased relative density and finer microstructure can be achieved for microwave-sintered specimens compared to samples made by traditional sintering methods [30].

3. Microwave-assisted production of zirconium diboride

In general, very limited articles have been published in the field of microwave sintering of ZrB_2. For example, by searching the terms "microwave sintering" and ZrB_2 or "zirconium diboride" in the titles, abstracts, and keywords of the published references, indexed in the Scopus citation database, only 17 documents were found in March 2023. This is probably due to the fact that ZrB_2 has electrical conductivity and the possibility of coupling microwave energy in it is limited [15, 32]. Anyway, in this article, an attempt has been made to review such limited published literature.

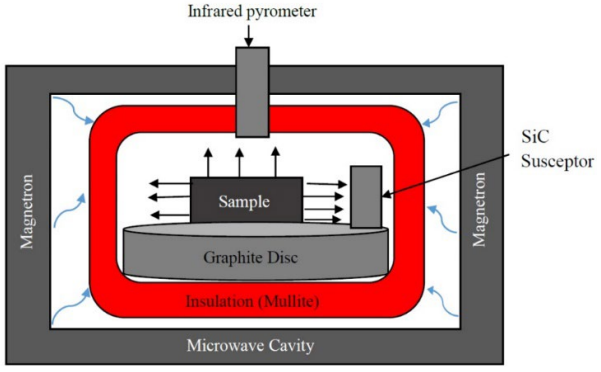

Fig. 1. Schematic sketch of the microwave sintering process. "© IOP Publishing. Reproduced with permission from Ref. [31]. All rights reserved".

3.1. Synthesis of ZrB_2 powders by microwave sintering

Deng et al. [33] synthesized ZrB_2 nano-particles via a polymer template route using boric acid, zirconyl, chitosan, and mannitol by microwave sintering in a furnace at 1300–1400 °C under an argon atmosphere. They studied the effects of the ratio Zr to B and C, processing temperature, and holding time on the purity of synthesized ZrB_2. Using the molar ratio of B/Zr/C=1/5.2/10, pure ZrB_2 was obtained. The optimum temperature and time for microwave sintering were 1320 °C and 1 h, respectively, to synthesize near spherical nano-powders (50 nm) [33].

Microwave heating was employed by Ding et al. [34] to synthesize ZrB_2 powders through the sol-gel route using zirconyl chloride octahydrate, citric acid, boric acid, and mannitol as the starting materials. They found that at the temperature of 1400 °C, the ZrB_2 powder can be completely synthesized via microwave heating technology, which was 300 °C less than the traditional options. At that temperature for 1 h by microwave, ultra-pure and ultra-fine ZrB_2 powders with near spherical morphology (1–2 μm) were successfully obtained using the B:Zr ratio of 2.77:1, and C:Zr ratio of 7.44:1 [34].

3.2. Sintering of ZrB_2-based ceramics by microwave sintering

3.2.1. Microwave sintering of ZrB_2–B_4C ceramics

Zhu et al. [35] fabricated two-phase ZrB_2–B_4C ceramic composites through microwave sintering of ZrB_2 powders with the addition of 4 wt% B_4C. The samples were sintered at 1630, 1720, 1820, and 1920 °C for 90 min in a multimode microwave applicator (2.45 GHz) with a heating rate of 50 °C /min and a cooling rate of 100 °C /min. B_4C addition promotes surface oxide removal from ZrB_2 powders. It should be noted that such oxides cause grain coarsening at high temperatures, which prevents full densification. Meanwhile, the addition of B_4C facilitates the microwave heating of ZrB_2 ceramic, due to the fact that B_4C is a microwave absorber, while ZrB_2 is an electrical conductor [35].

The sintered sample at 1630 °C reached a relative density of 88%, which indicates that this temperature was not enough for the complete densification of the material. By increasing the sintering temperature to 1720 °C, the relative density increased by 10% compared to the previous temperature and reached 98%. Reaching such a great relative density at a relatively low sintering temperature proved that the densification can be promoted using microwave sintering, at temperatures lower than those required for conventional sintering methods, without accelerating grain growth. Increasing the sintering temperature to 1820 °C caused an increase in the relative density to 99.5%, but further increasing the temperature to 1920 °C led to a slight decrease in this quantity. Therefore, the temperature of 1720 °C was sufficient and there was no special reason for increasing the temperature further [35].

The Vickers hardness values of the samples made at temperatures of 1630, 1720, 1820, and 1920 °C were reported as 10.5, 16.7, 17.5, and 15.45 GPa, respectively. Therefore, with the increase of the sintering temperature up to 1820 °C, the hardness trend was upward, but the further increase of the manufacturing temperature to 1920 °C led to a

drop in the hardness. Naturally, with the increase in sintering temperature, the relative density of the composites improved, and the amount of porosity decreased, and therefore the hardness obtained was higher. Due to the hexagonal structure and anisotropic thermal expansion of ZrB_2, the excessive increase in temperature up to 1920 °C caused the growth of grains; hence, during cooling it caused residual stresses and the formation of microcracks, which was the reason for the decrease in the hardness of the sample at the mentioned temperature [35].

The fracture toughness showed a different behavior and with increasing the processing temperature, it faced a further decrease, so that it decreased from 3.8 MPa.$m^{1/2}$ for the sample made at 1630 °C to 2.5 MPa.$m^{1/2}$ for the sample sintered at 1920 °C. The high fracture toughness in the sample with 12% porosity was attributed to the toughening mechanism of crack arresting by the pores. It seemed that the presence of secondary B_4C phase could not activate other toughening mechanisms such as crack deflection and crack bridging in the ZrB_2 microwave sintered ceramics [35].

3.2.2. Microwave sintering of ZrB_2–SiC ceramics

Similar to B_4C, SiC is also a beneficial absorber of microwave energy. Sharma and Karunakar [31] examined the effects of microwave sintering process parameters on the densification of ZrB_2–30 vol% SiC ceramics. They fabricated the composite samples at different sintering temperatures (1600–1900 °C), for various soaking times (30-50 min), with different heating rates (15–35 °C/min) in a microwave chamber with 3 kW power output and 2.45 GHz frequency under argon protection.

Microstructural investigation showed a homogeneous SiC dispensation in the microwave-sintered ZrB_2 matrix. In addition to the peaks of ZrB_2 and SiC as the main ingredients of the mixture, the phase analysis by X-ray diffraction (XRD) confirmed the peaks of ZrO_2 and B_4C in some samples, the former being due to the presence of impurities in the as-received ZrB_2 powder and the latter because of the possible reactions of boron with carbon. The ZrO_2 degraded the relative density and hardness, but the B_4C resulted in higher relative density and hardness [31].

A relatively dense sample with a relative density of 97.4% was achieved at 1800 °C, for 40 min with 15 °C/min heating rate. The relative density enhanced with increasing the sintering temperature up to 1800 °C but then dropped. In a similar trend, the relative density increased from the soaking time of 20 min to 40 min and then decreased. Such observations for relative density degradation were related to the high-temperature oxidation at prolonged soaking time. By increasing the heating rate, the relative density was decreased which might be attributed to the micro-cracking occurring due to the generation of residual stresses in the composite materials because of the difference in the thermal expansion coefficient of the constituents [31].

A Vickers hardness of 16.8 GPa was achieved at 1800 °C, for 40 min with 15 °C/min heating rate. The hardness enhanced with increasing the sintering temperature from 1600 to 1800 °C but then decreased. More residual stresses induced during cooling from a higher temperature and more porosity resulted in hardness degradation. The hardness increased as the soaking time increased from 30 to 40 min but then dropped for the time of 50 min. In addition, with increasing the heating rate, the hardness of the sintered composites decreased [31].

Among the composites sintered at various temperatures from 1600 to 1900 °C, the highest fracture toughness of 5.1 MPa.$m^{1/2}$ belonged to the sample developed at 1700 °C. The Vickers indentation impression, some cracks, and several toughening mechanisms detected in the sample sintered at 1700 °C for 40 min with 25 °C/min heating rate are presented in Fig. 2. Among the fabricated composites for soaking times of 30, 40, and 50 min, the maximum fracture toughness (4.7 MPa.$m^{1/2}$) belonged to the one sintered for 50 min. In fact, higher soaking time led to grain growth that acted as crack deflectors. Among the samples sintered with different heating rates of 15, 25, and 35 °C/min, the highest fracture toughness (4.4 MPa.$m^{1/2}$) was obtained with the heating rate of 15 °C/min. The greater heating rate resulted in micro-cracking during the cooling step [31].

In continuation, Sharma and Karunakar [36] studied the significance of input control factors of the microwave sintering process (sintering temperature, holding time, and heating rate) on the output responses of relative density, compressive strength, and hardness for ZrB_2–30 vol% SiC ceramics. The experiments were performed employing the Taguchi method (L9 orthogonal array). Analysis of variance (ANOVA) showed that all three input factors can significantly affect the relative density, hardness, and strength. However, the sintering temperature and soaking

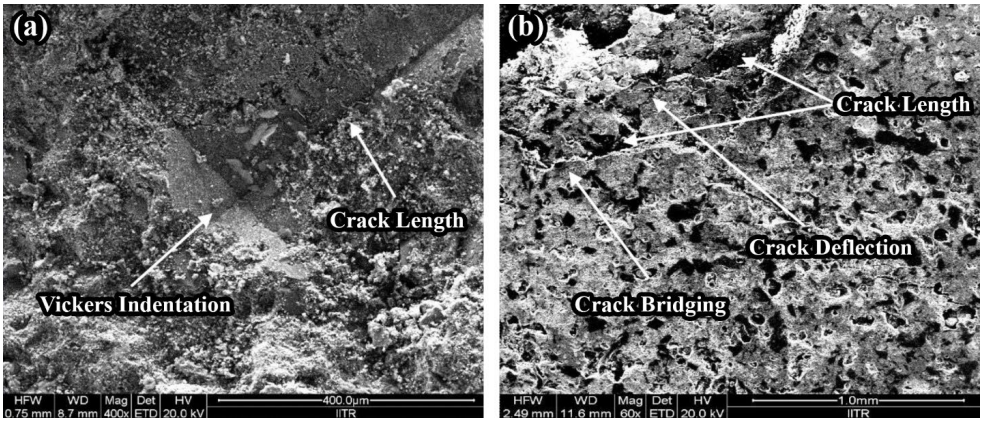

Fig. 2. a) Vickers indentation and b) cracks and toughening mechanisms in the ceramic sintered at 1700 °C for 40 min with a heating rate 25 °C/min. "© IOP Publishing. Reproduced with permission from Ref. [31]. All rights reserved".

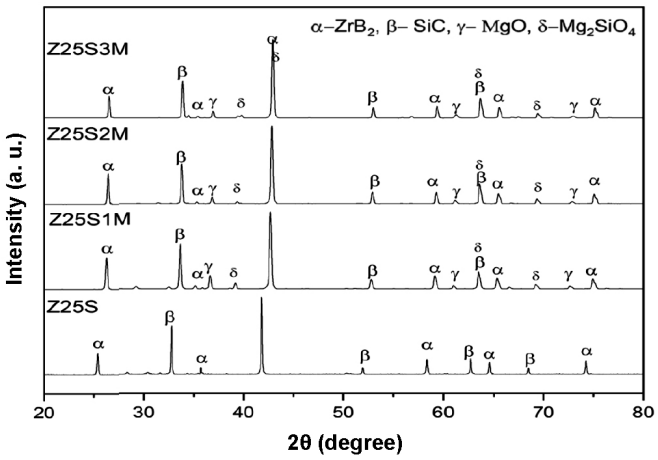

Fig. 3. XRD patterns of the microwave-sintered ZrB_2–SiC-based ceramics with different amounts of MgO additives. In naming the samples, the number before S indicates the amount of SiC and the number before M indicates the amount of MgO. "© Reproduced from Ref. [38] (J. Mater. Sci.) with permission from Springer Nature Customer Service Centre. All rights reserved. The Licensed Material is not part of the governing OA license but has been reproduced with permission".

time were the prime factors. The optimum microwave sintering conditions were 1850 °C temperature, 25 min soaking time, and 20 °C/min heating rate [36].

Wang et al. [37] prepared ZrB_2–SiC ceramics, reinforced by mixtures of SiC particles/whiskers, through microwave sintering. The SiC whiskers and SiC particles with a volume ratio of 1∶1 and total amounts of 0, 10, 20, and 30 vol% were added to the ZrB_2 matrix. The composites were densified in a microwave chamber at 1850 °C under argon protection with a power output of 1–10 kW and frequency of 2.45 GHz.

The ZrB_2 sample without additives reached a relative density of 94% after microwave sintering, and with the addition of SiC and increasing its amount, the relative density finally increased to 100% by adding a total of 30 vol% SiC. The researchers believed that the introduction of SiC enhanced the densification for the following reasons:

- As the microwave absorber during the heating step, SiC assisted in the densification of ZrB_2.
- Finer particles of SiC additives, both whiskers, and particulates, than the ZrB_2 matrix provided a better possibility to fill the grain boundaries.
- Eutectic reaction of SiO_2 (surface oxide impurity of SiC particles and whiskers) with ZrO_2 and B_2O_3 (surface oxide impurities of ZrB_2) removed such harmful layers. The eutectic reactions not only prevented grain coarsening of ZrB_2, but also boosted the sintering progress because of accelerated mass transfer in liquid phase.

Of course, it should be noted that only the first reason is exclusive to the microwave sintering process. The second and third reasons can be generalized for other processes as well [37].

Generally, the flexural strength enhanced with increasing SiC content, reaching a maximum of 625 MPa for ZrB_2–20 vol% SiC composite from 577 MPa for the monolithic SiC-free ceramic. Increased flexural strength by SiC addition was attributed to the boosted densification and grain refinement phenomena. Anyway, the flexural strength decreased to 540 MPa with the addition of 30 vol% SiC, due to the fine SiC particles/whiskers agglomeration [37].

The fracture toughness showed a similar increasing and then decreasing trend like the flexural strength. The lowest fracture toughness was obtained for the monolithic ZrB_2 sample (4.0 $MPa.m^{1/2}$) and the maximum value was measured for the composite containing 20 vol% SiC additive (7.2 $MPa.m^{1/2}$). The fracture toughness improvement was related to the activation of toughening mechanisms such as crack deflection, whiskers pull out, and crack branching. The drop in fracture toughness with the addition of 30 vol% SiC was attributed to the decrease in flexural strength and the reasons mentioned for it [37].

3.2.3. Microwave sintering of ZrB_2–SiC–MgO ceramics

Sharma and Karunakar [38] investigated the effect of MgO addition (1–3 vol%) on the ablation and mechanical properties of microwave-sintered ZrB_2–25 vol% SiC ceramics. The sintering process was carried out at 1800 °C for 40 min with a 15 °C/min heating rate under an argon atmosphere employing a microwave chamber with 3 kW power output and 2.45 GHz frequency.

The phase analysis by XRD identified the peaks of forsterite (Mg_2SiO_4) along with the ZrB_2, SiC, and MgO as the starting powders (Fig. 3). Reaction of SiO_2 and MgO led to the synthesis of Mg_2SiO_4 phase. The liquid phase formation due to the addition or formation of the secondary phases resulted in densification enhancement at relatively lower temperatures. In other words, the addition of MgO decreased the manufacturing temperature [38].

A uniform distribution dispersion of SiC and MgO was seen in the matrix of ZrB_2 up to the MgO amount of 2 vol%. Higher MgO additive resulted in the agglomeration and non-uniform dispersion of MgO in the ZrB_2–SiC microstructure. Generally, the introduction of MgO prevented extreme grain growth in the ZrB_2–SiC materials. The addition of 2 vol% MgO resulted in the maximum relative density due to the MgO pinning effect, but more additives dropped this characteristic because of the agglomeration and non-uniform distribution of MgO in the sintered samples [38].

The introduction of 2 vol% MgO led to the highest hardness. The porosities among the ZrB_2 matrix and SiC reinforcement phase led to

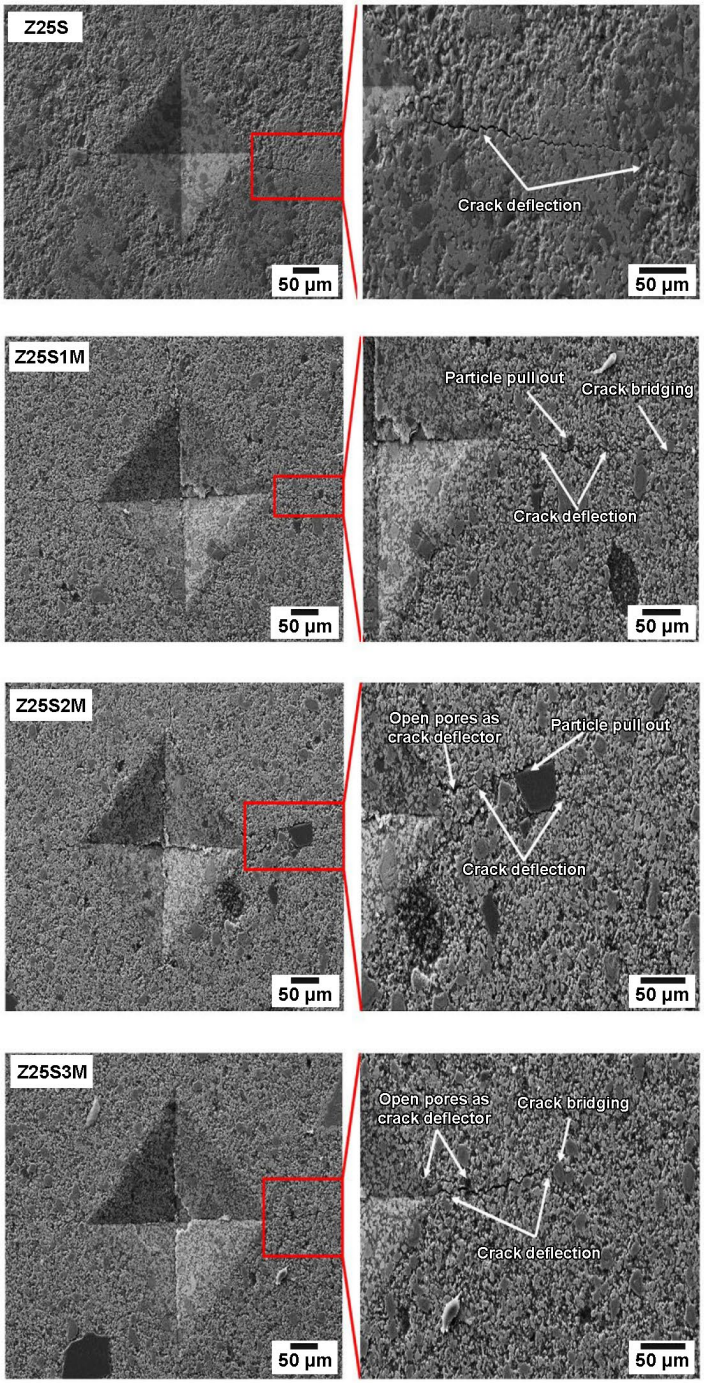

Fig. 4. Vickers indentation impressions and toughening mechanisms in the microwave-sintered ZrB_2–SiC-based ceramics with different amounts of MgO additives. In naming the samples, the number before S indicates the amount of SiC and the number before M indicates the amount of MgO. "© Reproduced from Ref. [38] (J. Mater. Sci.) with permission from Springer Nature Customer Service Centre. All rights reserved. The Licensed Material is not part of the governing OA license but has been reproduced with permission".

reduced hardness. The MgO addition intensified the fracture toughness of the composite materials as the maximum property was achieved with 3 vol% MgO. This sample showed the crack impeding because of the open pores. Anyway, the dominant toughening mechanisms were crack deflection, crack bridging, and particle pull-out (Fig. 4) [38].

The addition of MgO improved the ablation resistance and the samples with 2 vol% MgO showed the best performance against the ablation because of the synthesis of stable glassy layers of $MgZrSiO_4$ and Mg_2SiO_4, which acted as protective barriers against the oxygen diffusion. The ablation mechanism was also described by Sharma and Karunakar [38].

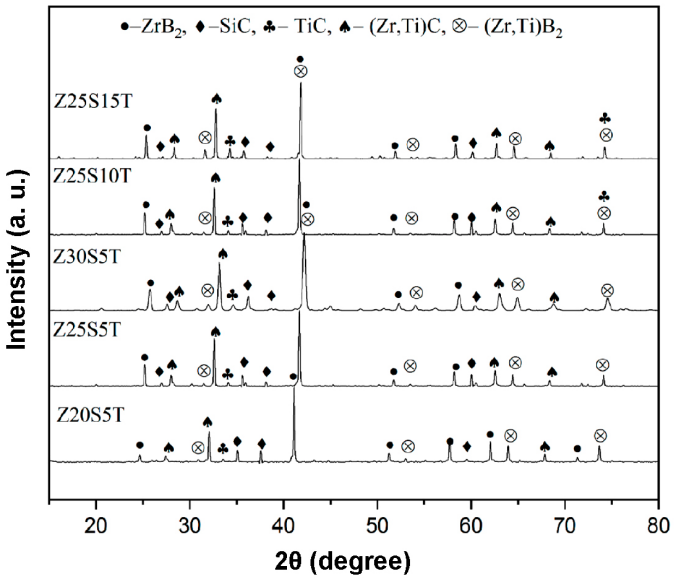

Fig. 5. XRD patterns of the microwave sintered ZrB_2–SiC–TiC ceramics with different amounts of carbide additives. In naming the samples, the number before S indicates the amount of SiC and the number before T indicates the amount of TiC. "© Reprinted from Ref. [39] with permission from Elsevier. All rights reserved".

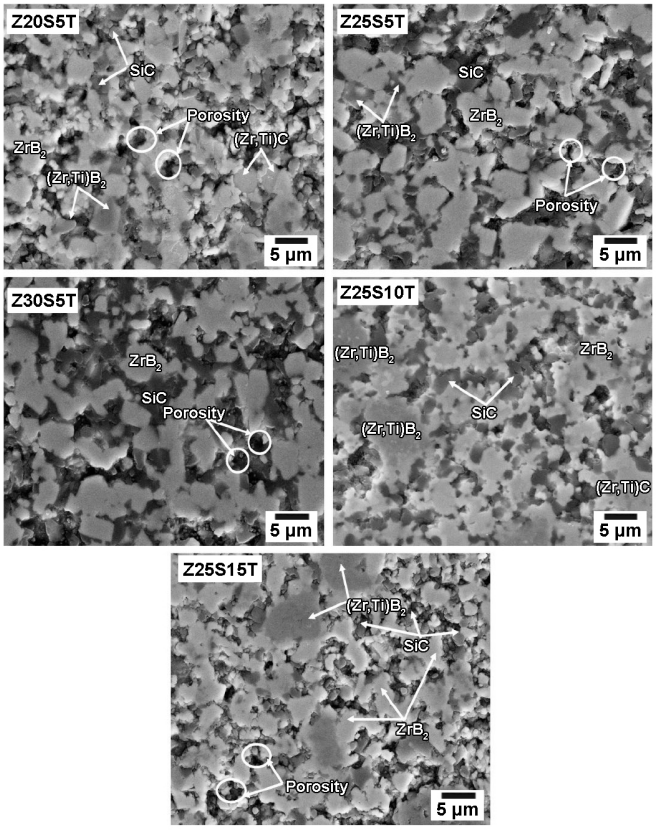

Fig. 6. Microstructures of the microwave sintered ZrB_2–SiC–TiC ceramics with different amounts of carbide additives. In naming the samples, the number before S indicates the amount of SiC and the number before T indicates the amount of TiC. "© Reprinted from Ref. [39] with permission from Elsevier. All rights reserved".

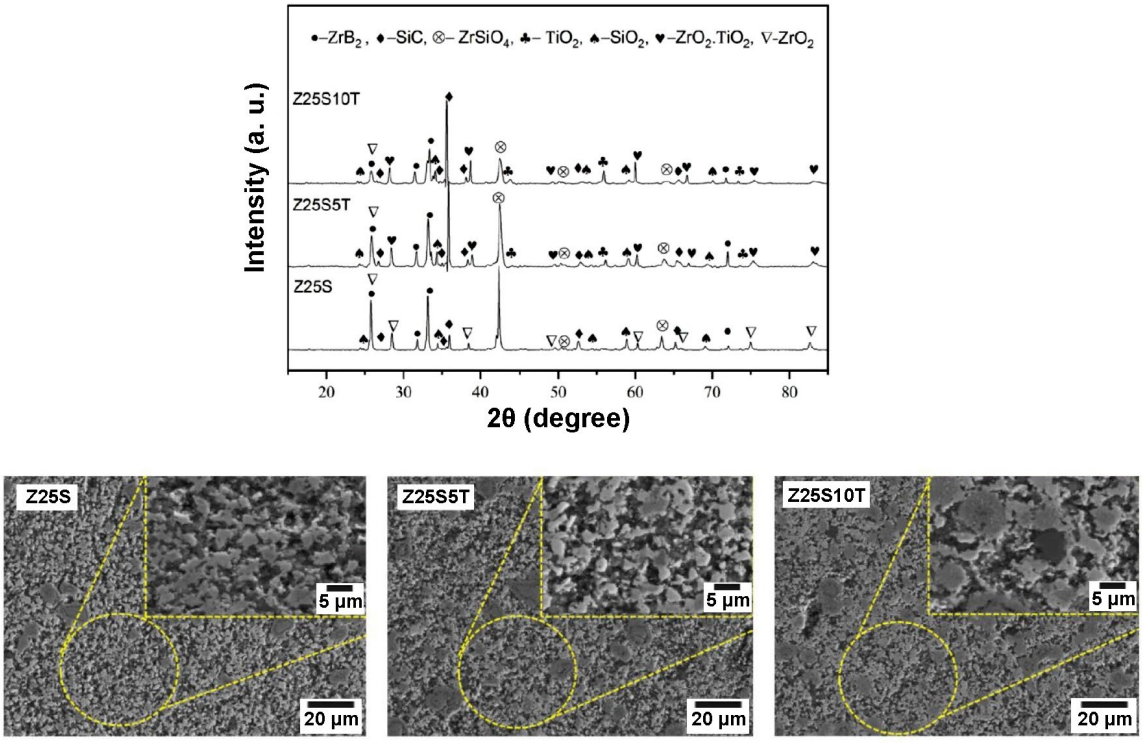

Fig. 7. FESEM micrographs of top surfaces and XRD patterns of the microwave-sintered ZrB_2–SiC–TiC ceramics with different amounts of carbide additives after ablation tests. In naming the samples, the number before S indicates the amount of SiC and the number before T indicates the amount of TiC. "© Reprinted from Ref. [41] with permission from Elsevier. All rights reserved".

3.2.4. Microwave sintering of ZrB_2–SiC–TiC ceramics

Sharma and Karunakar [39, 40] investigated the influences of the co-addition of SiC (20, 25, and 30 vol%) and TiC (5, 10, and 15 vol%) on the microstructure-properties correlations in the microwave-sintered ZrB_2-based ceramics. The samples were fabricated in a microwave sintering furnace with two 3-kW magnetrons at 1800 °C for 40 min with a 25 °C/min heating rate under argon protection to prevent oxidation.

Along with the main peaks of ZrB_2, TiC, and SiC, the in-situ synthesized solid solutions of (Zr,Ti)B_2 and (Zr,Ti)C were identified by the XRD analysis (Fig. 5). Moreover, no ZrO_2 peaks were detected in the sintered ceramics due to the possible reaction of ZrO_2 with TiC and the formation of (Zr,Ti)C [39].

The relative density increased with more addition of SiC from 20 to 25 vol% but then dropped with a further addition to 30 vol% because of the local formation of high-temperature regions around SiC that

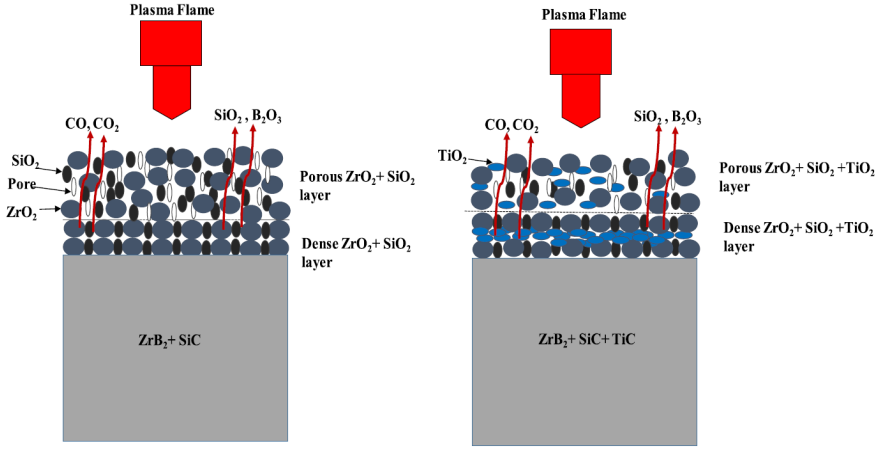

Fig. 8. Schematic representation of ablation mechanisms in the microwave-sintered ZrB_2–SiC and ZrB_2–SiC–TiC ceramics. "© Reprinted from Ref. [41] with permission from Elsevier. All rights reserved".

resulted in thermal runaways. Due to the non-uniform microwave heating, the developed thermal runaways in the sample led to residual porosity and micro-cracking. The addition of TiC caused a more homogenous microwave field and eliminated the thermal runaways. By increasing the TiC content from 5 to 10 vol%, the interconnectivity of SiC in the ZrB_2–SiC ceramics was reduced, which bested the sinterability. Further introduction of TiC to 15 vol% decreased the relative density because of the mismatch in the coefficients of thermal

Table 1. Density and mechanical properties of microwave sintered ZrB_2-based ceramics.

Composition	Sintering conditions	Relative density	Mechanical properties*	Ref.
ZrB_2–SiC 30 vol%	1600 °C/40 min/argon, heating rate: 25 °C/min	74.5%	HV: 10.1 GPa, K_{1C}: 4.8 MPa.m$^{1/2}$	[31]
	1700 °C/40 min/argon, heating rate: 25 °C/min	91.6%	HV: 11.4 GPa, K_{1C}: 5.1 MPa.m$^{1/2}$	
	1800 °C /40 min/argon, heating rate: 25 °C/min	96.0%	HV: 16.6 GPa, K_{1C}: 3.9 MPa.m$^{1/2}$	
	1900 °C/40 min/argon, heating rate: 25 °C/min	94.4%	HV: 13.2 GPa, K_{1C}: 3.9 MPa.m$^{1/2}$	
	1800 °C/30 min/argon, heating rate: 25 °C /min	96.0%	HV: 15.9 GPa, K_{1C}: 4.3 MPa.m$^{1/2}$	
	1800 °C/50 min/argon, heating rate: 25 °C/min	90.1%	HV: 13.2 GPa, K_{1C}: 4.7 MPa.m$^{1/2}$	
	1800 °C/40 min/argon, heating rate: 15 °C/min	97.4%	HV: 16.8 GPa, K_{1C}: 4.4 MPa.m$^{1/2}$	
	1800 °C/40 min/argon, heating rate: 35 °C/min	93.4%	HV: 12.6 GPa, K_{1C}: 4.2 MPa.m$^{1/2}$	
ZrB_2–B_4C 4 wt%	1630 °C/90 min/argon, heating rate: 50 °C/min	88.0%	HV: 10.5 GPa, K_{1C}: 3.8 MPa.m$^{1/2}$	[35]
	1720 °C/90 min/argon, heating rate: 50 °C/min	98.0%	HV: 16.7 GPa, K_{1C}: 3.2 MPa.m$^{1/2}$	
	1820 °C/90 min/argon, heating rate: 50 °C/min	99.5%	HV: 17.5 GPa, K_{1C}: 2.8 MPa.m$^{1/2}$	
	1920 °C/90 min/argon, heating rate: 50 °C/min	99.0%	HV: 15.4 GPa, K_{1C}: 2.5 MPa.m$^{1/2}$	
ZrB_2–SiC 30 vol%	1650 °C/25 min/argon, heating rate: 10 °C/min	83.4%	HV: 10.1 GPa, CS: 421 MPa	[36]
	1650 °C/35 min/argon, heating rate: 15 °C/min	85.6%	HV: 11.4 GPa, CS: 438 MPa	
	1650 °C/45 min/argon, heating rate: 20 °C/min	80.2%	HV: 10.9 GPa, CS: 452 MPa	
	1750 °C/25 min/argon, heating rate: 15 °C/min	94.0%	HV: 14.6 GPa, CS: 509 MPa	
	1750 °C/35 min/argon, heating rate: 20 °C/min	96.0%	HV: 16.4 GPa, CS: 651 MPa	
	1750 °C/45 min/argon, heating rate: 10 °C/min	94.4%	HV: 15.1 GPa, CS: 637 MPa	
	1850 °C/25 min/argon, heating rate: 20 °C/min	95.8%	HV: 15.9 GPa, CS: 683 MPa	
	1850 °C/35 min/argon, heating rate: 10 °C/min	96.1%	HV: 16.1 GPa, CS: 605 MPa	
	1850 °C/45 min/argon, heating rate: 15 °C/min	94.9%	HV: 15.4 GPa, CS: 586 MPa	
ZrB_2	1850 °C/argon	94.0%	FS: 577 MPa, K_{1C}: 4.0 MPa.m$^{1/2}$	[37]
ZrB_2–$SiC_{particle}$ 5 vol%–$SiC_{whisker}$ 5 vol%	1850 °C/argon	97.3%	FS: 614 MPa, K_{1C}: 6.1 MPa.m$^{1/2}$	[37]
ZrB_2–$SiC_{particle}$ 10 vol%–$SiC_{whisker}$ 10 vol%		98.6%	FS: 625 MPa, K_{1C}: 7.2 MPa.m$^{1/2}$	
ZrB_2–$SiC_{particle}$ 15 vol%–$SiC_{whisker}$ 15 vol%		100.0%	FS: 540 MPa, K_{1C}: 6.1 MPa.m$^{1/2}$	
ZrB_2–SiC 25 vol%	1800 °C/40 min/argon, heating rate: 15 °C/min	97.4%	HV: 13.0 GPa, K_{1C}: 5.1 MPa.m$^{1/2}$	[38]
ZrB_2–SiC 25 vol%–MgO 1 vol%	1800 °C/40 min/argon, heating rate: 15 °C/min	97.9%	HV: 15.0 GPa, K_{1C}: 5.6 MPa.m$^{1/2}$	[38]
ZrB_2–SiC 25 vol%–MgO 2 vol%		98.0%	HV: 15.9 GPa, K_{1C}: 6.3 MPa.m$^{1/2}$	
ZrB_2–SiC 25 vol%–MgO 3 vol%		97.6%	HV: 15.1 GPa, K_{1C}: 6.8 MPa.m$^{1/2}$	
ZrB_2–SiC 20 vol%–TiC 5 vol%	1800 °C/40 min/argon, heating rate: 25 °C/min	94.4%	HV: 15.7 GPa, FS: 522 MPa, CS: 306 MPa, K_{1C}: 5.9 MPa.m$^{1/2}$	[39]
ZrB_2–SiC 25 vol%–TiC 5 vol%		96.9%	HV: 19.2 GPa, FS: 549 MPa, CS: 319 MPa, K_{1C}: 5.7 MPa.m$^{1/2}$	
ZrB_2–SiC 30 vol%–TiC 5 vol%		96.3%	HV: 19.1 GPa, FS: 542 MPa, CS: 315 MPa, K_{1C}: 5.1 MPa.m$^{1/2}$	
ZrB_2–SiC 25 vol%–TiC 10 vol%		98.1%	HV: 21.8 GPa, FS: 597 MPa, CS: 326 MPa, K_{1C}: 6.1 MPa.m$^{1/2}$	
ZrB_2–SiC 25 vol%–TiC 15 vol%		96.1%	HV: 16.4 GPa, FS: 577 MPa, CS: 320 MPa, K_{1C}: 6.4 MPa.m$^{1/2}$	

* HV: Vickers hardness, CS: Compression strength, FS: Flexural strength, K_{1C}: Fracture toughness, (Note: the numbers in this table are rounded.)

expansion. The diffusion of TiC in the matrix of ZrB_2 was verified by microstructural investigations (Fig. 6) [39].

The mechanical properties such as hardness, compression strength, and flexural strength were boosted by increasing the SiC amount from 20 to 30 vol% in the ZrB_2 ceramics doped with 5 vol% TiC. Anyway, the fracture toughness dropped by increasing SiC content from 20 to 30 vol%. The mechanical performance was further boosted by the addition of more TiC from 5 to 15 vol% in the ZrB_2–25 vol% SiC specimens. The maximum relative density, hardness, and strength (flexural and compression) belonged to the ZrB_2–25 vol% SiC–10 vol% TiC sample, whereas the ceramic co-doped with 25 vol% SiC and 15 vol% TiC had the maximum fracture toughness [39].

Sharma and Karunakar [41] also studied the role of TiC addition (5–10 vol%) on the thermal shock resistance and ablation behavior of microwave-sintered ZrB_2–25 vol% SiC ceramics. The introduction of TiC led to the synthesis of TiO_2 and ZrO_2.TiO_2 films on the surface of oxidized ceramics (Fig. 7), which resulted in improved resistance against ablation and thermal shock. The schematic illustrations of the ablation mechanisms in TiC-free and TiC-doped ZrB_2–SiC composites are shown in Fig. 8. The improvement in thermal shock resistance was attributed to the high fracture toughness and flexural strength of the sintered ceramics [41].

The results obtained for the relative density and mechanical properties of different ZrB_2-based ceramics produced by the microwave sintering method in different conditions and with various additives are summarized in Table 1.

4. Concluding remarks

Among the interesting family of UHTCs, ZrB_2 is a non-oxide unique ceramic candidate for ultrahigh temperature applications specifically in the aerospace industry such as rocket nozzles, space shuttles, jet vanes, re-entry hypersonic vehicles, in addition to general applications like molten metal crucibles, parts in nuclear power plants, and high-temperature electrodes. For manufacturing appropriate ceramic parts, it seems necessary to select the best sintering method to reduce the defects and improve the properties as much as possible. Therefore, to develop dense ZrB_2 bulks with few defects, microwave sintering can be employed as an effective fabrication route to enhance the microstructural/mechanical characteristics compared to the conventional powder technology sintering techniques. The basics of the material and the process were reviewed in this paper in order to clarify the processing-densification-properties correlations in microwave-sintered ZrB_2-based UHTCs. The microwave-assisted production of zirconium diboride such as the synthesis of ZrB_2 powders as well as the sintering of bulk materials was also reviewed. Moreover, the roles of some carbides (B_4C, SiC, and TiC) and oxide (MgO) additive materials, based on the available published data in the literature, on the densification and mechanical behavior of ZrB_2 were summarized. Considering the importance of this process and the limited number of published papers, researchers can focus and pay more attention to the microwave sintering of ZrB_2 and its composites.

CRediT authorship contribution statement

Samira Savani: Investigation, Writing – original draft, Project administration, Supervision.
Mohammad Alipour: Conceptualization, Data curation.
Ankur Sharma: Resources, Writing – review & editing.
Dagarapu Benny Karunakar: Resources, Writing – review & editing.

Data availability

The data underlying this article will be shared on reasonable request to the corresponding author.

Declaration of competing interest

The authors declare no competing interests.

Funding and acknowledgment

The authors would like to thank Ramin Ahangar for valuable inputs and for fruitful discussions.

References

[1] N.P. Padture, Advanced structural ceramics in aerospace propulsion, Nat. Mater. 15 (2016) 804–809. https://doi.org/10.1038/nmat4687.
[2] J.S. Pelz, N. Ku, M.A. Meyers, L.R. Vargas-Gonzalez, Additive manufacturing of structural ceramics: a historical perspective, J. Mater. Res. Technol. 15 (2021) 670–695. https://doi.org/10.1016/j.jmrt.2021.07.155.
[3] B.R. Golla, A. Mukhopadhyay, B. Basu, S.K. Thimmappa, Review on ultra-high temperature boride ceramics, Prog. Mater. Sci. 111 (2020) 100651. https://doi.org/10.1016/j.pmatsci.2020.100651.
[4] A. Nisar, R. Hassan, A. Agarwal, K. Balani, Ultra-high temperature ceramics: Aspiration to overcome challenges in thermal protection systems, Ceram. Int. 48 (2022) 8852–8881. https://doi.org/10.1016/j.ceramint.2021.12.199.
[5] D. Ni, Y. Cheng, J. Zhang, J.-X. Liu, J. Zou, et al., Advances in ultra-high temperature ceramics, composites, and coatings, J. Adv. Ceram. 11 (2022) 1–56. https://doi.org/10.1007/s40145-021-0550-6.
[6] H. Mao, F. Shen, Y. Zhang, J. Wang, K. Cui, et al., Microstructure and mechanical properties of carbide reinforced TiC-based ultra-high temperature ceramics: A review, Coatings. 11 (2021) 1444. https://doi.org/10.3390/coatings11121444.
[7] J. Meng, H. Fang, H. Wang, Y. Wu, C. Wei, et al., Effects of refractory metal additives on diboride-based ultra-high temperature ceramics: A review, Int. J. Appl. Ceram. Technol. 20 (2023) 1350–1370. https://doi.org/10.1111/ijac.14336.
[8] M. Ghasilzadeh Jarvand, Z. Balak, Oxidation response of ZrB2–SiC–ZrC composites prepared by spark plasma sintering, Synth. Sinter. 2 (2022) 191–197. https://doi.org/10.53063/synsint.2022.24134.
[9] O. Uyanna, H. Najafi, Thermal protection systems for space vehicles: A review on technology development, current challenges and future prospects, Acta Astronaut. 176 (2020) 341–356. https://doi.org/10.1016/j.actaastro.2020.06.047.
[10] H.K.M. Al-Jothery, T.M.B. Albarody, P.S.M. Yusoff, M.A. Abdullah, A.R. Hussein, A review of ultra-high temperature materials for thermal protection system, IOP Conf. Ser. Mater. Sci. Eng. 863 (2020) 012003. https://doi.org/10.1088/1757-899X/863/1/012003.
[11] D. Bandivadekar, E. Minisci, Modelling and simulation of transpiration cooling systems for atmospheric re-entry, Aerospace. 7 (2020) 89. https://doi.org/10.3390/aerospace7070089.
[12] G. Akopov, M.T. Yeung, R.B. Kaner, Rediscovering the crystal chemistry of borides, Adv. Mater. 29 (2017) 1604506. https://doi.org/10.1002/adma.201604506.
[13] S.D. Oguntuyi, O.T. Johnson, M.B. Shongwe, Spark plasma sintering of ceramic matrix composite of ZrB2 and TiB2:

microstructure, densification, and mechanical properties—A review, Met. Mater. Int. 27 (2021) 2146–2159. https://doi.org/10.1007/s12540-020-00874-8.
[14] S.-Q. Guo, Densification of ZrB2-based composites and their mechanical and physical properties: a review, J. Eur. Ceram. Soc. 29 (2009) 995–1011. https://doi.org/10.1016/j.jeurceramsoc.2008.11.008.
[15] J.K. Sonber, A.K. Suri, Synthesis and consolidation of zirconium diboride: review, Adv. Appl. Ceram. 110 (2011) 321–334. https://doi.org/10.1179/1743676111Y.0000000008.
[16] M. Magnuson, L. Tengdelius, G. Greczynski, L. Hultman, H. Högberg, Chemical bonding in epitaxial ZrB2 studied by X-ray spectroscopy, Thin Solid Films. 649 (2018) 89–96. https://doi.org/10.1016/j.tsf.2018.01.021.
[17] D. Sciti, L. Silvestroni, V. Medri, F. Monteverde, Sintering and densification mechanisms of ultra-high temperature ceramics, Ultra-High Temperature Ceramics: Materials for Extreme Environment Applications, John Wiley & Sons, Inc, Hoboken. (2014) 112–143. https://doi.org/10.1002/9781118700853.ch6.
[18] W.G. Fahrenholtz, J. Binner, J. Zou, Synthesis of ultra-refractory transition metal diboride compounds, J. Mater. Res. 31 (2016) 2757–2772. https://doi.org/10.1557/jmr.2016.210.
[19] Z. Bahararjmand, M.A. Khalilzadeh, F. Saberi-Movahed, T.H. Lee, J. Wang, et al., Role of Si3N4 on microstructure and hardness of hot-pressed ZrB2−SiC composites, Synth. Sinter. 1 (2021) 34–40. https://doi.org/10.53063/synsint.2021.1113.
[20] S. Haghgooye Shafagh, S. Jafargholinejad, S. Javadian, Beneficial effect of low BN additive on densification and mechanical properties of hot-pressed ZrB2–SiC composites, Synth. Sinter. 1 (2021) 69–75. https://doi.org/10.53063/synsint.2021.1224.
[21] W.G. Fahrenholtz, G.E. Hilmas, I.G. Talmy, J.A. Zaykoski, Refractory diborides of zirconium and hafnium, J. Am. Ceram. Soc. 90 (2007) 1347–1364. https://doi.org/10.1111/j.1551-2916.2007.01583.x.
[22] F. Monteverde, S. Guicciardi, A. Bellosi, Advances in microstructure and mechanical properties of zirconium diboride based ceramics, Mater. Sci. Eng. A. 346 (2003) 310–319. https://doi.org/10.1016/S0921-5093(02)00520-8.
[23] J. Binner, M. Porter, B. Baker, J. Zou, V. Venkatachalam, et al., Selection, processing, properties and applications of ultra-high temperature ceramic matrix composites, UHTCMCs – a review, Int. Mater. Rev. 65 (2020) 389–444. https://doi.org/10.1080/09506608.2019.1652006.
[24] E.W. Neuman, B.J. Lai, J.L. Watts, G.E. Hilmas, W.G. Fahrenholtz, L. Silvestroni, Processing, microstructure, and mechanical properties of hot-pressed ZrB 2 ceramics with a complex Zr/Si/O-based additive, Int. J. Appl. Ceram. Technol. 18 (2021) 2224−2236. https://doi.org/10.1111/ijac.13866.
[25] F. Sadegh Moghanlou, M. Vajdi, M. Sakkaki, S. Azizi, Effect of graphite die geometry on energy consumption during spark plasma sintering of zirconium diboride, Synth. Sinter. 1 (2021) 54–61. https://doi.org/10.53063/synsint.2021.117.
[26] R. Hassan, K. Balani, Densification mechanism of spark plasma sintered ZrB2 and ZrB2-SiC ceramic composites, Mater. Charact. 179 (2021) 111320. https://doi.org/10.1016/j.matchar.2021.111320.
[27] H. Istgaldi, M. Mehrabian, F. Kazemi, B. Nayebi, Reactive spark plasma sintering of ZrB2-TiC composites: Role of nano-sized carbon black additive, Synth. Sinter. 2 (2022) 67–77. https://doi.org/10.53063/synsint.2022.22107.
[28] C.-N. Sun, M.C. Gupta, Laser sintering of ZrB2, J. Am. Ceram. Soc. 91 (2008) 1729–1731. https://doi.org/10.1111/j.1551-2916.2008.02369.x.
[29] J.D. Ford, D.C.T. Pei, High temperature chemical processing via microwave absorption, J. Microw. Power. 2 (1967) 61–64. https://doi.org/10.1080/00222739.1967.11688647.
[30] D.E. Clark, W.H. Sutton, Microwave processing of materials, Annu. Rev. Mater. Sci. 26 (1996) 299–331. https://doi.org/10.1146/annurev.ms.26.080196.001503.
[31] A. Sharma, D.B. Karunakar, Development and investigation of densification behavior of ZrB2–SiC composites through microwave sintering, Mater. Res. Express. 6 (2019) 105072. https://doi.org/10.1088/2053-1591/ab3aca.
[32] M. Oghbaei, O. Mirzaee, Microwave versus conventional sintering: A review of fundamentals, advantages and applications, J. Alloys Compd. 494 (2010) 175–189. https://doi.org/10.1016/j.jallcom.2010.01.068.
[33] Q.H. Deng, Z.H. Ding, X.F. Shen, S.Y. Du, Q. Huang, Synthesis of ultra-fine zirconium diboride powders by polymer template method following by microwave sintering, Key Eng. Mater. 697 (2016) 49–53. https://doi.org/10.4028/www.scientific.net/KEM.697.49.
[34] Z. Ding, X. Huang, W. Liu, I.J. Kim, Y.-H. Han, Preparation of high-temperature active zirconium boride powders via precursor route and microwave sintering, Adv. Appl. Ceram. 120 (2021) 222–226. https://doi.org/10.1080/17436753.2021.1933839.
[35] S. Zhu, W.G. Fahrenholtz, G.E. Hilmas, S.C. Zhang, E.J. Yadlowsky, M.D. Keitz, Microwave sintering of a ZrB2–B4C particulate ceramic composite, Compos. Part A Appl. Sci. Manuf. 39 (2008) 449–453. https://doi.org/10.1016/j.compositesa.2008.01.003.
[36] A. Sharma, D.B. Karunakar, Parametric optimization of ZrB2–SiC composites sintered through microwave sintering using grey relational Taguchi, Adv. Sci. Eng. Med. 12 (2020) 1328–1333. https://doi.org/10.1166/asem.2020.2598.
[37] H.-L. Wang, C.-A. Wang, D.-L. Chen, H.-L. Xu, H.-X. Lu, et al., Preparation and characterization of ZrB2-SiC ultra-high temperature ceramics by microwave sintering, Front. Mater. Sci. China. 4 (2010) 276–280. https://doi.org/10.1007/s11706-010-0091-3.
[38] A. Sharma, D.B. Karunakar, Influence of MgO addition on mechanical and ablation characteristics of ZrB2–SiC composites developed through microwave sintering, J. Mater. Sci. 56 (2021) 17979–17993. https://doi.org/10.1007/s10853-021-06287-1.
[39] A. Sharma, D.B. Karunakar, Effect of SiC and TiC addition on microstructural and mechanical characteristics of microwave sintered ZrB2 based hybrid composites, Ceram. Int. 47 (2021) 26455–26464. https://doi.org/10.1016/j.ceramint.2021.06.058.
[40] A. Sharma, D.B. Karunakar, Comparative evaluation of microstructural and mechanical properties of microwave and spark plasma sintered ZrB2-SiC-TiC composites, J. Mater. Eng. Perform. 31 (2022) 576–589. https://doi.org/10.1007/s11665-021-06204-2.
[41] A. Sharma, D.B. Karunakar, Influence of TiC addition on ablation and thermal shock behaviour of microwave sintered ZrB2–SiC–TiC composites, Ceram. Int. 48 (2022) 34504–34515. https://doi.org/10.1016/j.ceramint.2022.08.031.